JOURNAL OF VIROLOGY, Aug. 1995, p. 4727–4736 Vol. 69, No. 8
0022-538X/95/$04.00+0

Mutational Analysis of Vaccinia Virus Nucleoside Triphosphate Phosphohydrolase II, a DExH Box RNA Helicase

CHRISTIAN H. GROSS AND STEWART SHUMAN*

Molecular Biology Program, Sloan-Kettering Institute, New York, New York 10021

Received 6 March 1995/Accepted 24 April 1995

Vaccinia virus nucleoside triphosphate phosphohydrolase II (NPH-II), a 3′-to-5′ RNA helicase, displays sequence similarity to members of the DExH family of nucleic acid-dependent nucleoside triphosphatases (NTPases). The contributions of the conserved GxGKT and DExH motifs to enzyme activity were assessed by alanine scanning mutagenesis. Histidine-tagged versions of NPH-II were expressed in vaccinia virus-infected BSC40 cells and purified by nickel affinity and conventional fractionation steps. Wild-type His-NPH-II was indistinguishable from native NPH-II with respect to RNA helicase, RNA binding, and nucleic acid-stimulated NTPase activities. The K-191→A (K191A), D296A, and E297A mutant proteins bound RNA as well as wild-type His-NPH-II did, but they were severely defective in NTPase and helicase functions. The H299A mutant was active in RNA binding and NTP hydrolysis but was defective in duplex unwinding. Whereas the NTPase of wild-type NPH-II was stimulated >10-fold by polynucleotide cofactors, the NTPase of the H299A mutant was nucleic acid independent. Because the specific NTPase activity of the H299A mutant in the absence of nucleic acid was near that of wild-type enzyme in the presence of DNA or RNA and because the K_m for ATP was unaltered by the H299A substitution, we regard this mutation as a "gain-of-function" mutation and suggest that the histidine residue in the DExH box is required to couple the NTPase and helicase activities.

Vaccinia virus encodes an essential RNA helicase that catalyzes unidirectional unwinding of 3′-tailed duplex RNAs in the presence of a divalent cation and any common nucleoside triphosphates (NTPs) or deoxy-NTPs (dNTPs) (31, 32). The vaccinia virus helicase (known previously as NTP phosphohydrolase II [NPH-II]) is a member of the DExH family of RNA-dependent nucleoside triphosphatases (NTPases) (24, 31, 32). The DExH family is defined by several conserved motifs arrayed in a collinear fashion; the spacing between the motifs varies among the family members (11, 14, 29). The first motif, GxxGxGKT, corresponds to the Walker A nucleotide binding motif commonly seen in NTPases; the signature motif DExH is a variant of the Walker B box (39). Vaccinia virus helicase most closely resembles the PRP16, PRP2, and PRP22 proteins of *Saccharomyces cerevisiae*, which are involved in mRNA splicing (3–5); the *Drosophila* MLE protein, which is implicated in dosage compensation of transcription (16); and human RNA helicase A (20). The size of the DExH family continues to expand as the signature motifs are observed in newly cloned genes. Typically, such gene products are designated putative helicases in the absence of supporting biochemical data. An intrinsic DNA-dependent or RNA-dependent NTPase activity has been demonstrated for many DExH proteins, including bacterial RecQ, RecG, and PriA (21, 22, 38, 40); yeast PRP16, PRP2, SNF2/SWI2, RAD3, and RAD25 (12, 13, 18, 30, 37); human helicase A (19) and ERCC2 (35); vaccinia virus NPH-I, NPH-II, and early transcription factor (2, 25); and plum pox virus CI (17). Several of these proteins have been shown to be true helicases. The vaccinia virus NPH-II, human helicase A, and potyvirus CI enzymes are RNA helicases (17, 19, 31), whereas RecQ, RecG, PriA, RAD3, ERCC2, and RAD25 are DNA helicases (12, 21, 22, 35, 37, 38, 40).

Although membership in the DExH family, or in the related DEAD box family (11, 29), can guide biochemical studies once a new gene is cloned, the conserved motifs neither ensure nor exclude the existence of an associated helicase activity. More important, even among the family members that actually are helicases, sequence motif conservation has no predictive value regarding the key biochemical properties of the protein, i.e., directionality, NTP specificity, and nucleic acid specificity. For example, within the DExH family, RAD3 is a 5′-to-3′ DNA helicase dependent strictly on ATP or dATP (37), whereas vaccinia virus helicase and human helicase A are 3′-to-5′ RNA helicases activated promiscuously by any NTP (19, 31, 32).

Mutational analysis of representative helicase family members can provide useful insights into the function of the conserved structural motifs. Among the RNA helicases, structure-function studies have been pursued most intensively for eIF-4A, the prototypical DEAD box protein (26, 27). In this paper, we present structure-function studies of vaccinia virus RNA helicase, a DExH box protein, via targeted mutagenesis and biochemical characterization of the mutated proteins. Our findings underscore the role of the conserved GKT and DExH motifs in NTP hydrolysis but not in RNA binding. Mutation of the histidine residue of the DExH box impairs RNA unwinding and renders the NTPase constitutively active in the absence of a polynucleotide cofactor. Thus, RNA binding and NTP hydrolysis are necessary, but not sufficient, for helicase activity.

MATERIALS AND METHODS

Cells and viruses. BSC40 cells were maintained in Dulbecco's modified Eagle's medium (DME) supplemented with 5% fetal bovine serum. HuTK$^-$143 cells were grown in DME with 10% fetal bovine serum. Wild-type vaccinia virus WR and vTF7-3, a recombinant virus that expresses bacteriophage T7 RNA polymerase (8), were propagated in BSC40 cells at 37°C.

Construction of a T7-based NPH-II expression vector. An 853-bp *Bam*HI-*Hin*dIII fragment from a vaccinia virus genomic *Hin*dIII-I plasmid and a 3,854-bp *Hin*dIII-*Bgl*II fragment from a genomic *Hin*dIII-G plasmid were cloned in tandem into a modified pBS vector (Stratagene) containing a *Bgl*II site in the polylinker. The resulting plasmid, pBSNPH-II, contained the complete I8 gene encoding NPH-II. A unique *Nde*I site was introduced at the translation initiation codon by site-directed mutagenesis (15). An *Nde*I-*Bgl*II fragment containing the I8 gene was inserted into the T7-based expression plasmid pET14b (Novagen) to generate pET-His-NPH-II. In this plasmid, a 60-nucleotide leader sequence

* Corresponding author.

containing six tandem histidine codons was fused in frame to the 5′ end of the NPH-II gene. The entire NPH-II expression cassette was excised with *Sca*I and *Bgl*II and inserted into a pBS(−) plasmid digested with *Hin*cII and *Bam*HI. A *Bgl*II site was created in this plasmid immediately 3′ of the NPH-II translation termination codon by site-directed mutagenesis. A 2,099-bp *Nco*I-*Bgl*II fragment containing the complete histidine-tagged NPH-II gene was then inserted into the T7-based eukaryotic expression plasmid pTM1 (7), which had been digested with *Nco*I and *Bam*HI. The resulting pTM-His-NPH-II plasmid contained the NPH-II gene under the control of a T7 promoter and a picornavirus cap-independent translational enhancer (7).

Coinfection expression system. A recombinant vaccinia virus containing the T7-His-NPH-II expression cassette inserted into the vaccinia virus thymidine kinase (TK) gene was constructed by electroporation of pTM-His-NPH-II into BSC40 cells infected with vaccinia virus WR. After electroporation, the infected cells were resuspended in 25 ml of DME and an aliquot (4 ml) was placed on a virgin BSC40 monolayer. Cells were harvested after incubation at 37°C for 48 h. Recombinant viruses were selected by plaque assay on HuTK$^-$ cell monolayers in the presence of bromodeoxyuridine (25 μg/ml). After three rounds of plaque purification, TK$^-$ virus recombinants were amplified and the insertion of the T7-His-NPH-II cassette into the TK gene was confirmed by diagnostic PCR. To achieve expression of His-NPH-II, 15 confluent BSC40 cell monolayers (350-cm^2 dishes) were shifted from 37 to 31°C approximately 12 h prior to coinfection with vTF7-3 and vHis-NPH-II at a multiplicity of 10 for each virus. Infected cells were incubated at 31°C. After 24 h, the medium was removed and cells were washed with methionine-free DME and then overlaid with (per dish) 10 ml of methionine-free DME containing 6.6 μCi of [L-^{35}S]methionine (>800 Ci/mmol) per ml. The medium was removed after 4 h and replaced with fresh methionine-free DME. Cells were then harvested with a Teflon scraper. The suspension was centrifuged, and the cell pellet was resuspended in 20 ml of buffer B (20 mM Tris [pH 8.0], 10 mM NaCl) and stored at −80°C.

Purification of wild-type His-NPH-II. Cells harvested after coinfection with vTF7-3 and vHis-NPH were lysed by freezing and thawing in hypotonic buffer B. All subsequent operations were performed at 4°C. The suspension was adjusted to 0.3 M NaCl, 10% glycerol, 0.1% Triton X-100, and 0.1 mM phenylmethylsulfonyl fluoride and then subjected to 10 15-s bursts of sonication. Insoluble material was removed by centrifugation at 20,000 × *g* for 30 min. The supernatant was mixed with 1 ml of nickel-nitrilotriacetic acid-agarose resin (Qiagen) that had been equilibrated with buffer C (20 mM Tris HCl [pH 8.0], 300 mM NaCl, 10% glycerol, 0.1% Triton X-100). The slurry was rotated continuously for 1 h and then poured into a column and washed with 40 ml of buffer C followed by 40 ml of 5 mM imidazole in buffer C. The column was eluted stepwise with 2 ml of buffer C containing 50, 100, and 500 mM imidazole. The polypeptide composition of the column fractions was monitored by sodium dodecyl sulfate-polyacrylamide gel electrophoresis (SDS-PAGE) (with protein detection by Coomassie blue staining and by autoradiography). His-NPH-II was recovered in the 50 mM imidazole eluate. This fraction was diluted threefold with buffer A (50 mM Tris HCl [pH 8.0], 2 mM dithiothreitol, 1 mM EDTA, 10% glycerol, 0.1% Triton X-100) and then applied to a 2-ml phosphocellulose column that had been equilibrated with buffer A. The column was eluted stepwise with buffer A containing 0.1, 0.2, 0.3, 0.4, 0.5, and 0.6 M NaCl. His-NPH-II eluted in the 0.3 and 0.4 M NaCl steps. An aliquot (0.25 ml) of the 0.4 M NaCl fraction was applied to a 4.7-ml 15 to 30% glycerol gradient containing 0.5 M NaCl in buffer A and then centrifuged for 18 h at 55,000 rpm in a Beckman SW55 rotor. Fractions (0.17 ml) were collected from the bottom of the tube. Protein standards were sedimented in a parallel gradient.

Enzyme assays. ATPase activity was assayed in the presence of nucleic acid cofactor [either poly(C) or single-stranded M13mp18 DNA] as the release of $^{32}P_i$ from [γ-^{32}P]ATP as described previously (33). RNA helicase reaction mixtures (20 μl) contained 40 mM Tris HCl (pH 8.0), 2 mM dithiothreitol, 1 mM $MgCl_2$, 1 mM ATP, and 25 fmol of [α-^{32}P]GMP-labeled standard double-stranded RNA (dsRNA) substrate (32). After incubation for 15 min at 37°C, reactions were halted by addition of 5 μl of 0.1 M Tris HCl (pH 7.4)–5 mM EDTA–0.5% SDS–50% glycerol–0.1% xylene cyanol–0.1% bromophenol blue. Aliquots (20 μl) were applied to an 8% polyacrylamide gel containing 0.5× Tris-borate-EDTA and electrophoresed at a 15-mA constant current. Labeled RNAs were visualized by autoradiographic exposure of the dried gel. RNA binding reaction mixtures (20 μl) contained 40 mM Tris HCl (pH 8.0), 2 mM dithiothreitol, 1 mM $MgCl_2$, and 25 fmol of [α-^{32}P]GMP-labeled single-stranded RNA (ssRNA) (98-mer, prepared as described previously [19, 32]). After incubation for 15 min at 37°C, samples were adjusted to 8% glycerol and 20-μl aliquots were electrophoresed through a native 8% polyacrylamide gel containing 0.25× Tris-borate-EDTA at a 15-mA constant current. Labeled RNAs were visualized by autoradiography of the dried gel. The extent of RNA-protein complex formation was quantified with a Fuji BAS1000 Bio-imaging analyzer or via scintillation counting of excised gel slices.

Substrates. Radiolabeled standard dsRNA helicase substrate was prepared as described previously (19). In brief, the RNA strands were transcribed in vitro from linear plasmid templates by using SP6 RNA polymerase. The 38-mer strand of the duplex substrate (5′-GAAUACACG<u>GAAUUCGAGCUCGCCCGGGGAUCCUCUAG</u>-3′) was radiolabeled to a high specific activity with [α-^{32}P]GTP. The partially complementary 98-nucleotide strand (5′-GAAUACAAGCUUGGGCUGCAGGUCGACU<u>CUAGAGGAUCCCCGGGCGAGCUCGAAUUC</u>GGGUCUCCCUAUAGUGAGUCGUAUUAAUUUCGAUAAGCCAG-3′) was labeled with [α-^{32}P]GTP at a 300-fold-lower specific activity. (The duplex region is underlined.) The transcription reaction products were subjected to urea-PAGE; radiolabeled transcripts were localized by autoradiography and recovered from an excised gel slice. Strand annealing was performed at a 2:1 molar ratio of 98-mer to 38-mer. The tailed RNA duplexes were then purified by native gel electrophoresis (19).

Alanine mutagenesis of His-NPH-II. Phagemid pTM-His-NPH-II contains the His-tagged NPH-II gene under the control of a T7 promoter and a picornavirus cap-independent translational enhancer (7). Uracil-substituted single-stranded pTM-His-NPH-II DNA was used as a template for oligonucleotide-directed mutagenesis (15). Mutagenic DNA primers were designed to create alanine substitutions at residues K-191, D-296, E-297, and H-299 in the GxGKT and DExH motifs of His-NPH-II. The presence of the desired mutations was screened for initially by the gain or loss of a restriction site and was confirmed by DNA sequencing. The entire NPH-II gene was sequenced in each case.

Transient transfection expression system. Confluent BSC40 cell monolayers (350-cm^2 dish), maintained in DME supplemented with 5% fetal bovine serum, were shifted from 37 to 31°C approximately 12 h prior to infection with vTF7-3 virus (8) at a multiplicity of 10. At 1 h postinfection, the medium was removed and cells were dislodged by treatment with 0.05% trypsin–0.53 mM EDTA. Suspended cells were mixed with 20 ml of DME and recovered by centrifugation for 5 min at 4°C in a clinical centrifuge. The pellet was washed with 5 ml of HBS (20 mM HEPES [*N*-2-hydroxyethylpiperazine-*N*′-2-ethanesulfonic acid, pH 7.0], 150 mM NaCl, 0.7 mM Na_2HPO_4, 5 mM KCl, 6 mM glucose) and centrifuged as before. The pellet was resuspended in 0.8 ml of cold HBS, transferred to a tube containing 20 μg of pTM-His-NPH-II plasmid DNA (encoding either wild-type or Ala-substituted alleles of His-NPH-II), and chilled on ice for 10 min. The contents of the tube were transferred to a chilled Bio-Rad 0.4-cm electrode gap cuvette, which was pulsed at 200 V (capacitance, 960 μF) with a Bio-Rad Gene Pulser equipped with a Bio-Rad Capacitance Extender, and then placed on ice for 10 min. The transfected cells were mixed with 25 ml of DME and then plated on a fresh 150-mm-diameter dish. After 24 h at 31°C, the medium was removed and cells were washed with methionine-free DME and then overlaid with 10 ml of methionine-free DME containing 6.6 μCi of [L-^{35}S]methionine (>800 Ci/mmol) per ml. The medium was removed after 4 h and replaced with fresh methionine-free DME. Cells were then harvested with a Teflon scraper. The suspension was centrifuged, and cell pellet was resuspended in 1 ml of buffer B.

Purification of His-NPH-Ala mutant proteins. Cells harvested after transfection with pTM-His-NPH-II-Ala plasmids were thawed on ice, adjusted to 0.3 M NaCl, 10% glycerol, 0.1% Triton X-100, and 0.1 mM phenylmethylsulfonyl fluoride, and then subjected to 10 15-s bursts of sonication. The 20,000 × *g* supernatant was mixed with 100 μl of nickel-nitrilotriacetic acid-agarose resin in a 1.5-ml microcentrifuge tube for 1 h with continuous rotation. The resin was recovered by centrifugation, and the supernatant fraction was removed. The resin was then resuspended in 1 ml of buffer C, recentrifuged, and subjected to three more cycles of washing with buffer C followed by four 1-ml washes with 5 mM imidazole in buffer C. Bound protein was eluted stepwise with buffer C containing 50, 100, and 500 mM imidazole. His-NPH-II-Ala was recovered in the 50 and 100 mM imidazole fractions. The 100 mM imidazole fractions, which, for each mutant, had a polypeptide composition similar to that of the 0.4 M phosphocellulose fraction of wild type His-NPH-II (see Fig. 3), were purified further by sedimentation through 4.7-ml 15 to 30% glycerol gradients containing 0.5 M NaCl in buffer A. The gradients were centrifuged for 18 h at 55,000 rpm in a Beckman SW55 rotor. Fractions (0.17 ml) were collected from the bottom of the tube.

Construction of His_{10}-NPH-II expression vectors. A 2,039-bp *Nde*I-*Xho*I fragment from pTM-His-NPH-II or pTM-His-NPH-II(H299A) containing the complete wild-type or H-299→A (H299A) mutant coding sequence was inserted into the T7-based expression plasmid pET16b (Novagen). This maneuver fused the NPH-II gene in frame to a 63-nucleotide 5′ leader sequence encoding 10 tandem His residues. A 2,102-bp *Nco*I-*Xho*I fragment containing each His_{10}-NPH-II allele was then reinserted into pTM1 that had been digested with *Nco*I and *Xho*I. The H299A mutation was confirmed by DNA sequencing. A recombinant virus containing the wild-type His_{10}-NPH-II allele inserted into the TK locus was constructed as described above. The wild-type His_{10}-NPH-II protein was expressed in BSC40 cells by coinfection as described above for the His_6-NPH-II protein. The His_{10}-NPH-II(H299A) mutant protein was expressed by plasmid transfection of vTF7-3 infected cells as described above.

Purification of His_{10}-NPH-II. Wild-type His_{10}-NPH-II was purified essentially as described for His_6-NPH-II with some modifications. After adsorption to Ni-agarose, the column was washed with 50 mM imidazole in buffer C (three 8-ml fractions), this was followed by two 3-ml washes with buffer C containing 500 mM imidazole. The His_{10}-NPH-II protein was recovered in the first 500 mM imidazole fraction, as assessed by Coomassie blue staining or autoradiography following SDS-PAGE. His_{10}-NPH-II(H299A) was expressed by using the transient transfection system as described above. Transfection of cells with the pTM1 vector served as a control. His_{10}-NPH-II(H299A) was purified by Ni-agarose chromatography, and the protein was recovered in the 500 mM imidazole eluate. Aliquots of the 500 mM imidazole fraction were further purified by glycerol gradient sedimentation as described above.

Anti-NPH-II serum. Polyclonal rabbit antiserum was prepared against a carboxyl-truncated version of the NPH-II protein (amino acids 1 to 645) isolated from the insoluble fraction of lysates of *Escherichia coli* BL21(DE3) that had been induced to overexpress the protein encoded by a pET-NPH-II(1-645) plasmid. Insoluble polypeptides were resolved by preparative SDS-PAGE. The NPH-II(1-645) antigen was eluted from an excised gel slice. Immunization was performed at Pocono Rabbit Farm and Laboratory, Canadensis, Pa. The specificities of the preimmune and immune sera were determined by Western blot (immunoblot) analysis against the original antigen and against other truncated versions of the NPH-II protein produced in *E. coli.*

RESULTS

Expression of recombinant vaccinia virus RNA helicase. Our efforts to express the full-length NPH-II polypeptide in *E. coli* by using a T7-based system were unsuccessful insofar as little or no protein of the appropriate size was detected upon induction (not shown). Amino- and carboxyl-truncated versions of NPH-II were expressed at high levels in bacteria, but the proteins were always insoluble (not shown). We therefore elected to express NPH-II under the control of a T7 promoter in cultured mammalian cells infected with a vaccinia virus (vTF7-3) that expresses T7 RNA polymerase (7). To aid in protein purification, the NPH-II gene was altered by addition of a sequence encoding an amino-terminal leader peptide containing six consecutive histidines. This allows affinity purification based on the adherence of His-tagged proteins to an immobilized nickel resin. Affinity purification is critical for structure-function studies, in which mutated versions of the vaccinia virus helicase expressed under T7 control must be resolved from the "native" NPH-II encoded by the genomic I8 gene and driven by vaccinia virus promoters.

His-NPH-II protein expression was achieved either by transfection of the expression plasmid pTM-His-NPH-II into vTF7-3-infected cells or by coinfection of BSC40 cells with vTF7-3 and a vaccinia virus recombinant, vT7-NPH, containing the T7-based His-NPH-II expression cassette integrated into the virus TK gene. The latter method was convenient for the expression of wild-type His-NPH-II, whereas the transfection technique was employed for the expression of mutated versions of the helicase. (We avoided using recombinant viruses carrying mutated His-NPH-II genes because of the potential for reversion of the mutation by gene conversion from the endogenous NPH-II gene.) We found that the solubility of expressed His-NPH-II protein was enhanced when the cells were maintained at 31°C during the infection. Metabolic labeling with [^{35}S]methionine prior to harvesting the infected cells helped in gauging His-NPH-II expression and solubility and allowed us to track the radiolabeled His-NPH-II polypeptide during subsequent purification steps.

Purification and characterization of wild-type His-NPH-II. Soluble lysates of cells coinfected with vTF7-3 and vT7-NPH were subjected to nickel-agarose affinity chromatography. Whereas most proteins did not adsorb to the resin, a select group of polypeptides were retained and were eluted by 50 mM imidazole (Fig. 1A; compare lanes FT and 50 mM). Protein labeling with [^{35}S]methionine at 24 h postinfection was limited primarily to vaccinia virus-encoded late polypeptides and to the His-NPH-II protein. Most radiolabeled soluble proteins were recovered in the unbound fraction during nickel chromatography (Fig. 1B, lane FT). A single ^{35}S-labeled 70-kDa polypeptide was eluted at 50 mM imidazole; this species corresponded to the prominent 70-kDa protein observed in the Coomassie blue-stained gel. Other stained polypeptides in the 50 mM imidazole fraction, which were not metabolically labeled, were presumed to be of host cell origin. The 70-kDa species, which represents His-NPH-II, was not detected in the bound fraction when lysates of cells infected with vTF-3 alone were subjected to nickel affinity chromatography (not shown). (Note that the calculated molecular mass of His-NPH-II [based on the amino acid sequence] is 80 kDa, but the protein migrates more rapidly than expected during SDS-PAGE. It was noted previously that native NPH-II purified from virions also migrated more rapidly during SDS-PAGE than expected from its calculated molecular mass [31].)

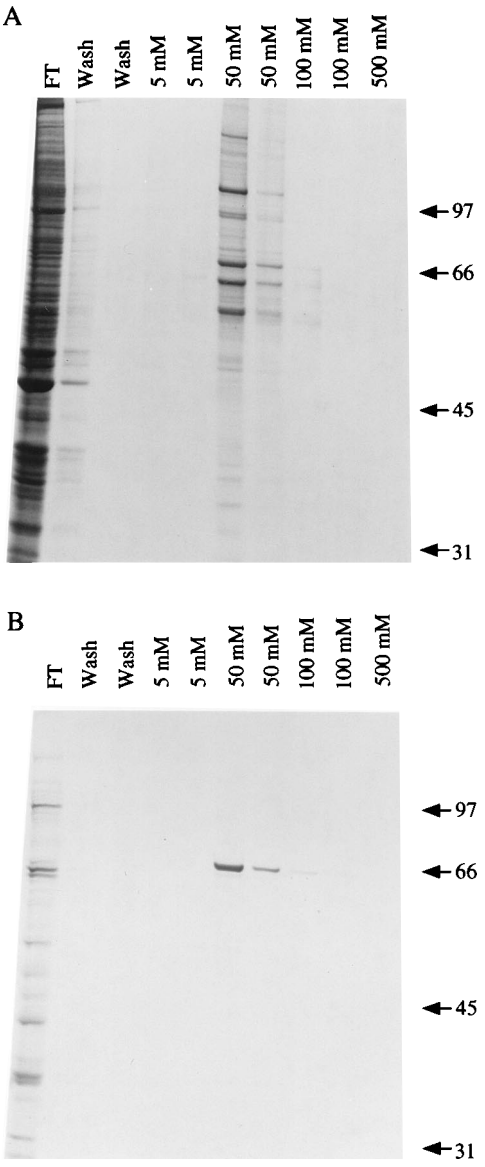

FIG. 1. Nickel affinity chromatography of His-NPH-II. The soluble lysate from coinfected BSC40 cells was chromatographed on Ni-nitrilotriacetic acid-agarose as described in Materials and Methods. The polypeptide compositions of the column flowthrough (FT) (50-μl aliquot) and of the wash and sequential imidazole eluates (75 μl of each fraction) were analyzed by SDS-PAGE, and polypeptides were visualized by staining with Coomassie blue (A). The gel was then dried under vacuum, and ^{35}S-labeled polypeptides were visualized by autoradiography (B). The positions and sizes (in kilodaltons) of marker proteins are indicated at the right by arrows.

His-NPH-II (from the 50 mM imidazole fraction) was adsorbed to phosphocellulose and was step eluted at 300 and 400 mM NaCl (Fig. 2). The partitioning of the ^{35}S-labeled polypeptide in the 300 and 400 mM fractions was identical to that of the Coomassie blue-stained 70-kDa protein (not shown). The

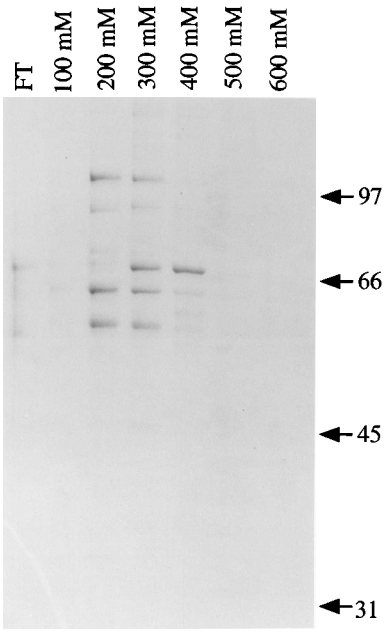

FIG. 2. Phosphocellulose chromatography of His-NPH-II. Phosphocellulose chromatography was performed as described in Materials and Methods. Aliquots (75 μl) of the flowthrough (FT) and the indicated NaCl eluate fractions were analyzed by SDS-PAGE. A Coomassie blue-stained gel is shown. The positions and sizes (in kilodaltons) of marker proteins are indicated at the right by arrows.

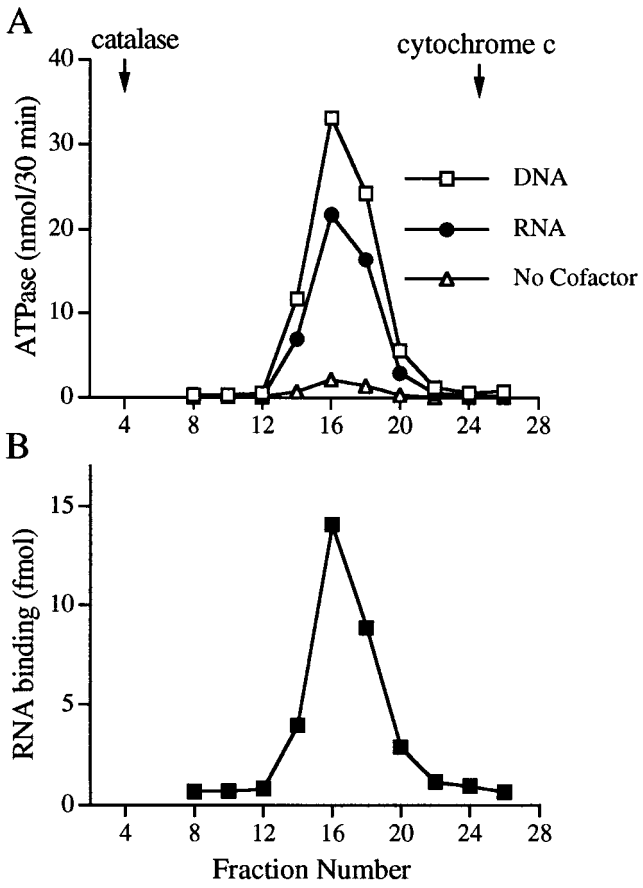

FIG. 3. Glycerol gradient sedimentation of His-NPH-II. An aliquot of the 0.4 M NaCl phosphocellulose fraction was sedimented in a glycerol gradient as described in Materials and Methods. (A) Aliquots (4 μl) of the indicated glycerol gradient fractions were assayed for ATPase activity in the presence of M13mp18 ssDNA (□) or poly(C) (●) cofactor and in absence of nucleic acid (△). ATPase is expressed as nanomoles of $^{32}P_i$ released from [γ-^{32}P]ATP during a 30-min incubation at 37°C. The positions of reference proteins centrifuged in a parallel gradient are indicated by the arrows. The direction of sedimentation is from right to left. (B) Fractions from the same glycerol gradient were assayed for RNA binding (see Fig. 4A). The amount of labeled RNA present in the protein-RNA complex was quantitated with a Phosphorimager.

chromatographic behavior of His-NPH-II was distinct from that of the major contaminating proteins, which eluted from phosphocellulose in the 200 and 300 mM NaCl fractions.

A single peak of nucleic acid-dependent NTPase activity was detected when the 0.4 M phosphocellulose fraction was sedimented in a glycerol gradient (Fig. 3A). The ATPase activity profile correlated with the abundance of the 70-kDa His-NPH-II polypeptide (not shown). ssDNA or ssRNA was an effective cofactor for the ATPase. Activity in the absence of exogenous polynucleotides was 6 to 10% of that observed in the presence of ssDNA (Fig. 3A). The nucleic acid cofactor specificities for the recombinant ATPase were the same as that reported for native NPH-II purified from vaccinia virus virions. A characteristic of the native enzyme is the ability to bind single-stranded nucleic acids in the absence of nucleotides (31, 32). Incubation of His-NPH-II with a radiolabeled 98-mer ssRNA resulted in the formation of a discrete protein-RNA complex that was resolved from free RNA during native gel electrophoresis (Fig. 4A). The RNA binding activity profile across the glycerol gradient coincided with that of the nucleic acid-dependent ATPase (Fig. 3). RNA binding by native NPH-II has been shown to be proportional to the amount of protein added to the reaction mixture (31, 32). From knowledge of the molar concentration of input RNA and assuming that the gel-shifted species contained one "functional unit" of protein bound to one molecule of RNA, the molar concentration of enzyme (i.e., as "RNA binding units") in the peak glycerol gradient fraction was estimated (by titration of RNA binding versus amount of input enzyme) to be 14 nM. (We cannot state definitively whether the functional unit of NPH-II bound to RNA is a monomer or a dimer of the NPH-II polypeptide.)

Helicase activity was tested with the standard substrate described previously (19, 31). This tailed dsRNA consists of a 98-nucleotide RNA hybridized to a 38-nucleotide radiolabeled RNA to produce a tailed molecule with a 29-bp duplex region. His-NPH-II unwound the dsRNA molecule in the presence of ATP (Fig. 4B). The labeled product of the helicase reaction comigrated during electrophoresis with the single-stranded species obtained by thermal denaturation of the substrate (Fig. 4B, lane Δ). The RNA-unwinding activity cosedimented with ATPase activity. The NTP requirement for helicase activity of His-NPH-II was satisfied by any one of the eight common ribo-NTPs or dNTPs (data not shown). Helicase activity also required a divalent cation. Effective cofactors were Mg, Co, and Mn, whereas Ca, Cu, and Zn failed to activate the helicase (data not shown). These nucleotide and divalent cation requirements were identical to those found for the RNA helicase purified from vaccinia virus virions (31).

Expression and purification of mutated His-NPH-II proteins. Alanine substitution mutations of the His-tagged NPH-II protein were introduced at residues within conserved motifs I and III, specifically, at Lys-191 in the GxGKT element and at Asp-296, Glu-297, and His-299 in the DEVH motif. Alanine scanning provides a simple approach to assess the essentiality of a given amino acid for protein function, in that

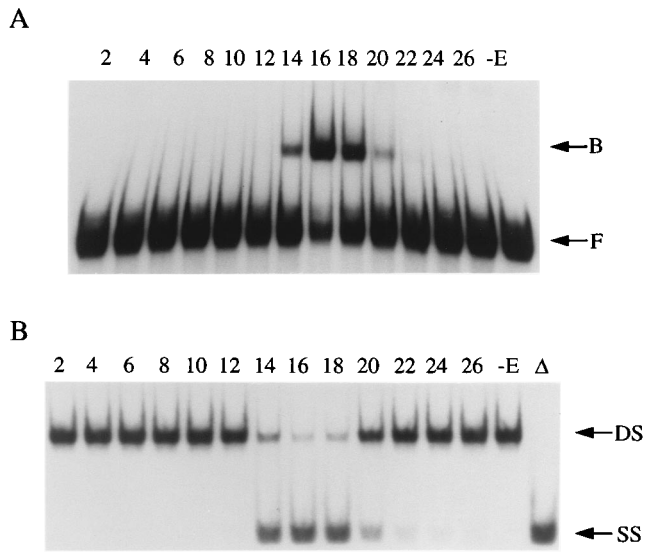

FIG. 4. Cosedimentation of RNA binding and helicase activities. (A) Aliquots (1 μl) of the indicated glycerol gradient fractions were assayed for RNA binding as described in Materials and Methods. The fraction numbers are indicated above the lanes. A control reaction lacking added protein is shown in lane −E. The positions of the protein-bound (B) and free (F) 98-mer RNAs are indicated at the right by arrows. (B) Glycerol gradient fractions were diluted 10-fold in buffer A, and 1-μl aliquots were assayed for RNA-unwinding activity as described in Materials and Methods. The fraction numbers are indicated above the lanes. A control reaction lacking added protein is shown in lane −E. A sample containing RNA substrate that was denatured by heating at 95°C for 5 min followed by cooling on ice is shown in lane Δ. The positions of the dsRNA substrate (DS) and released ssRNA (SS) are indicated at the right by arrows.

alanine substitution eliminates the side chain beyond the β carbon yet usually does not alter the main-chain conformation or impose extreme electrostatic or steric effects (1, 6, 10). Expression of the mutant proteins was achieved by transfection of pTM-His-NPH-II-Ala plasmids into vTF7-3-infected BSC40 cells (7, 8). Infected BSC40 cells transfected with the pTM1 vector served as a control. Metabolic labeling with [^{35}S]methionine prior to harvesting the infected cells helped in gauging His-NPH-II expression and solubility and allowed us to track the radiolabeled His-NPH-II polypeptide during subsequent purification steps. Nickel-agarose chromatography facilitated purification of the His-tagged proteins from soluble cell lysates. His-NPH-II-Ala proteins recovered in the 100 mM imidazole eluate were purified further by glycerol gradient sedimentation.

All four His-NPH-II-Ala proteins sedimented as discrete peaks as indicated by the RNA binding activity profile (Fig. 5) and by the distribution of ^{35}S-labeled NPH-II polypeptide across the gradients (not shown). All four mutant proteins retained the ability to form a complex with ssRNA; the electrophoretic mobility of the RNA-protein complex formed by the mutant His-NPH-II proteins was similar to that of the wild-type enzyme (Fig. 5). To verify that the RNA binding detected in these gradients was attributable to His-NPH-II, a control extract from pTM1-transfected cells was chromatographed on nickel-agarose and the 100 mM imidazole fraction was sedimented in parallel with the His-NPH-II-Ala fractions. No RNA-protein complex comparable to the His-NPH-II–RNA complex was detected (Fig. 5, Mock).

RNA binding by His-NPH-II mutants. The amounts of the shifted protein-RNA complex formed by wild-type His-NPH-II and by each of the Ala mutants varied linearly with the amount of input enzyme up to 20 fmol of complex formation. The

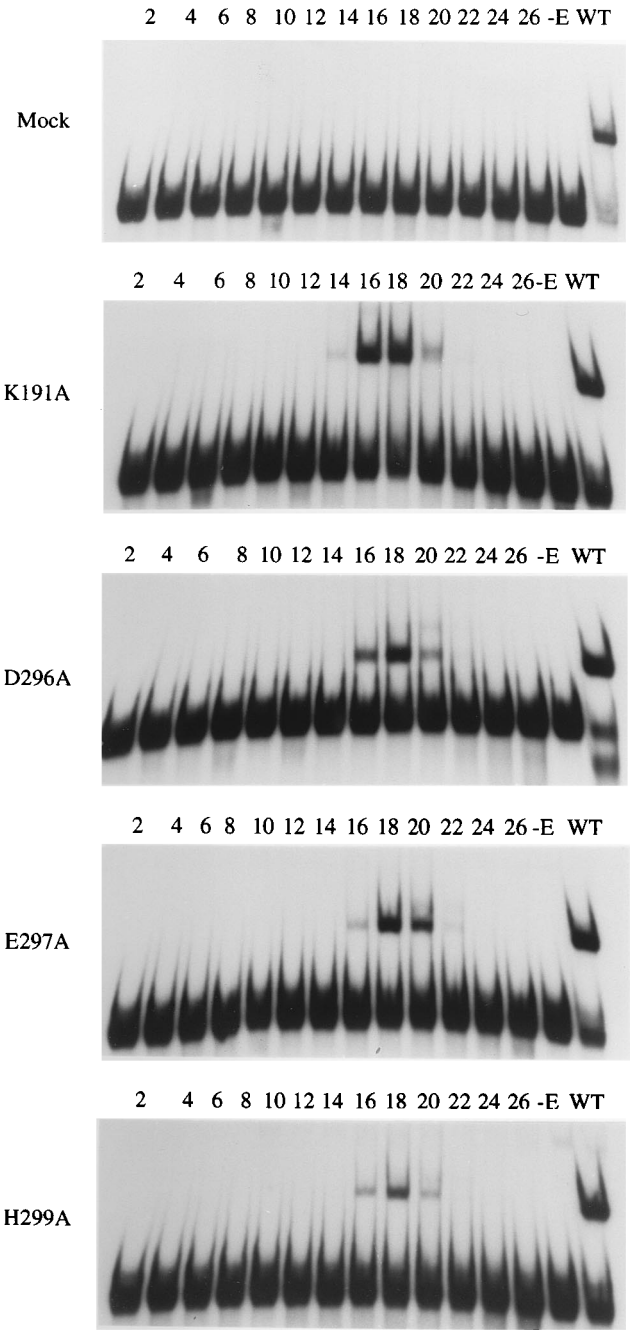

FIG. 5. RNA binding assays of His-NPH-II-Ala mutant proteins sedimented through a glycerol gradient. Preparations of the indicated mutant His-NPH-II-Ala proteins and corresponding fractions from mock-transfected cells were sedimented in glycerol gradients as described in Materials and Methods. Aliquots (1 μl) of the gradient fractions were assayed for RNA binding. The fraction numbers are indicated above the lanes. The direction of sedimentation was from right to left; lower-number fractions represent more rapidly sedimenting material. A negative control reaction lacking added protein (−E) and a positive control containing purified wild-type His-NPH-II (WT) were included in each series.

concentrations of His-NPH-II, expressed as RNA binding units, in the peak glycerol gradient fractions of each Ala mutant and of wild-type His-NPH-II, determined by titrating the protein samples within the linear range of the assay, were as follows: wild type, 14 nM; K191A mutant, 9 nM; D296A mutant, 6 nM; E297A mutant, 7 nM; and H299A mutant, 3 nM.

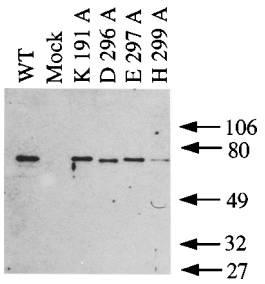

FIG. 6. Western blot analysis of wild-type and mutated NPH-II proteins. Aliquots (12 μl) of the peak glycerol gradient fractions (fraction 18 for Ala-substituted proteins; see Fig. 5) were electrophoresed through an 8% polyacrylamide gel containing 0.1% SDS. Proteins were transferred electrophoretically to a nitrocellulose membrane that was blocked in TBST buffer (10 mM Tris-HCl [pH 8.0], 150 mM NaCl, 0.05% Tween 20) containing 5% bovine serum albumin and 1% dry milk. Membranes were incubated for 2 h at room temperature with rabbit anti-NPH-II serum diluted 1:6,000 in TBST. After removal of serum and washing with TBS–Tween 0.4%, bound antibodies were localized by incubation with anti-rabbit immunoglobulin conjugated with horseradish peroxidase. Immunoreactive polypeptides were visualized with an enhanced chemiluminescence system (ECL; Amersham) according to the instructions of the manufacturer. The positions and sizes (in kilodaltons) of coelectrophoresed prestained protein markers are indicated on the right. WT, wild type.

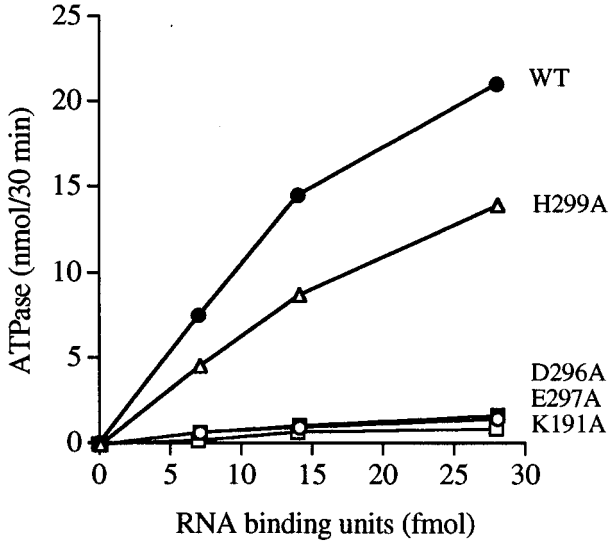

FIG. 7. ATP hydrolysis by wild-type and mutant His-NPH-II proteins as a function of enzyme concentration. Peak glycerol gradient fractions were assayed for ATPase activity in the presence of M13mp18 ssDNA cofactor. ATPase is expressed as nanomoles of $^{32}P_i$ released from [γ-^{32}P]ATP during a 30-min incubation at 37°C and is plotted as a function of input enzyme (as RNA binding units; 1 U binds 1 fmol of ssRNA). The source of the protein preparation is indicated next to each curve. WT, wild type.

The relative amounts of His-NPH-II polypeptide in each peak glycerol gradient fraction were assessed by Western blotting (Fig. 6). Aliquots (12 μl) of the peak glycerol gradient fractions from the wild-type and each of the His-NPH-II-Ala protein preparations and from the equivalent fraction from the mock-transfected preparation were resolved by SDS-PAGE, transferred to nitrocellulose, and probed with antiserum against NPH-II expressed in bacteria. A 72-kDa immunoreactive polypeptide was apparent in the wild-type and each of the mutant His-NPH-II samples. No immunoreactive species was detected in the mock-transfected sample (Fig. 6). Densitometric scanning of the Western blot indicated that the concentrations of immunoreactive K191A, D296A, E297A, and H299A mutant proteins were 80, 60, 70, and 20% of that of the wild-type His-NPH-II protein, respectively. These results correlate with the relative RNA binding activities and support the conclusion that interaction of His-NPH-II with RNA was unaffected by the alanine substitutions in the GKT and DExH motifs.

Mutational effects on ATPase activity. ATPase activity in the presence of a DNA cofactor was assayed across each of the glycerol gradients. A low level of ATPase cosedimented with RNA binding activity in the K191A, D296A, and E297A preparations (not shown). No peak of ATPase activity was detected in the glycerol gradient of the mock-transfected preparation (not shown). In contrast, the H299A protein displayed a robust level of ATPase that cosedimented with the RNA binding activity.

The extent of ATP hydrolysis by the peak glycerol gradient NPH-II fractions during a 30-min incubation in the presence of a DNA cofactor was proportional to the amount of input enzyme, expressed as RNA binding units (Fig. 7). The specific ATPase activities of the K191A, E297A, and D296A mutants were reduced to about 1/20 of the activity of wild-type His-NPH-II. In contrast, the specific activity of the H299A mutant was 60% of that of the wild-type enzyme. Thus, the histidine residue in the DExH box was not essential for NTP hydrolysis.

Titrations of the K191A, E297A, and D296A mutants in the absence of a polynucleotide cofactor indicated that the phosphohydrolase activity of these proteins was stimulated three- to fourfold by nucleic acid (not shown). Quite surprisingly, the omission of nucleic acid had almost no effect on ATP hydrolysis by the H299A mutant (see below).

Helicase activity of mutated His-NPH-II proteins. Duplex RNA unwinding was assessed as a function of enzyme concentration for the wild-type and Ala-substituted His-NPH-II proteins (Fig. 8). The extent of strand displacement was proportional to the level of input wild-type enzyme in the range of 0.07 to 0.28 RNA binding unit and neared saturation at >0.7 RNA binding unit (Fig. 9). We estimated that wild-type His-NPH-II displaced 70 molecules of RNA duplex per RNA binding unit. All four mutant proteins displayed reduced levels of helicase activity (Fig. 8 and 9). RNA unwinding by the E297A, K191A, and D296A mutants increased with the amount of input protein, and saturation was achieved in each case at about 3 RNA binding units, albeit with a much lower overall yield of displaced RNA than with wild-type His-NPH-II. Paradoxically, the H299A mutant, which retained ATPase activity, displayed the lowest level of RNA unwinding (Fig. 8 and 9). We confirmed for all four mutant protein preparations that the observed helicase activity was completely dependent on exogenous NTP and that any of the four ribo-NTPs was sufficient for RNA unwinding (data not shown). The helicase activity profiles across each glycerol gradient coincided with those of RNA binding and ATPase activities (not shown). RNA helicase activity was lacking in the glycerol gradient of the mock-transfected preparation (not shown).

For the K191A, D296A, and E297A mutants, the magnitude of the mutational effect on helicase activity mirrored the decrement in ATPase activity. However, the H299A protein was nearly fully competent for ATP hydrolysis but was severely compromised with respect to strand displacement. Thus, ATP hydrolysis, while necessary for RNA unwinding, was clearly not sufficient.

Further characterization of the effects of the H299A substitution on ATPase activity. To confirm and extend the initial finding that the H299A mutant was constitutively active for ATPase without a polynucleotide cofactor, we reconstructed the expression vectors such that the NPH-II polypeptide was fused to an amino-terminal leader peptide containing 10 con-

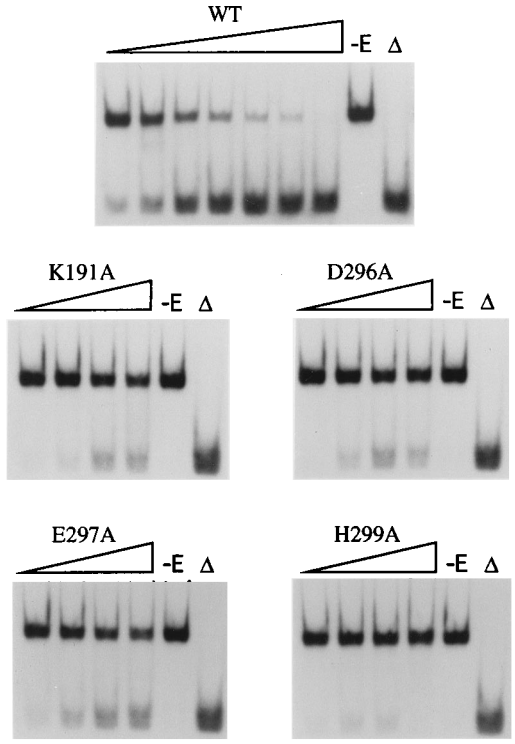

FIG. 8. RNA unwinding by wild-type and mutant His-NPH-II proteins. Helicase assay mixtures contained 25 fmol of standard dsRNA substrate and increasing amounts of enzyme, expressed as RNA binding units. The titration series for wild type (WT) His-NPH-II (glycerol gradient fraction) contained (from left to right) 0.07, 0.14, 0.28, 0.7, 1.4, 2.8, and 7 RNA binding units. Each titration series for His-NPH-II mutant proteins (glycerol gradient fractions) contained (from left to right) 0.7, 1.4, 2.8, and 7 RNA binding units. Enzyme was omitted from control reactions (−E). A sample containing heat-denatured RNA substrate is shown in lane Δ.

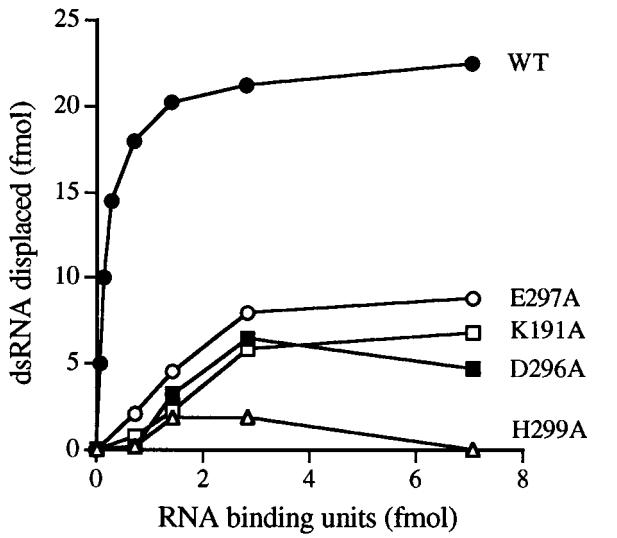

FIG. 9. RNA unwinding by wild-type and mutant His-NPH-II proteins as a function of enzyme concentration. The extent of unwinding for each reaction in Fig. 8 was quantitated with a Phosphorimager. The amount of RNA displaced is plotted as a function of input enzyme (as RNA binding units; 1 U binds 1 fmol of ssRNA). The source of the protein preparation is indicated next to each curve. WT, wild type.

secutive His residues. The additional His residues afforded tighter binding of His_{10}-NPH-II to the Ni-agarose resin, such that the column could be washed extensively with 50 mM imidazole; this was followed by elution of His_{10}-NPH-II with 500 mM imidazole. The 500 mM eluate was virtually homogeneous with respect to the His_{10}-NPH-II polypeptide (not shown). His_{10}-NPH-II(H299A) was purified similarly, except that the Ni column was washed with 100 mM imidazole before the His_{10}-NPH-II(H299A) protein was eluted with the 500 mM imidazole fraction (not shown). The affinity-purified wild-type His_{10}-NPH-II and His_{10}-NPH-II(H299A) preparations were analyzed by glycerol gradient sedimentation. Gradient fractions were assayed for ATP hydrolysis in the presence of DNA or RNA cofactors and in the absence of nucleic acid. A single peak of ATPase activity was observed for the wild-type protein (not shown); this activity was strongly stimulated by either DNA or RNA. The H299A mutant also sedimented as a single peak of ATPase activity; however, there was little effect of DNA or RNA on ATP hydrolysis (see below). RNA binding activity, as assessed by gel shift, paralleled ATPase activity for both proteins. Western blot analysis of the gradient profile confirmed that the activity peak coincided with the abundance of the immunoreactive NPH-II polypeptide (not shown). Sedimentation of the 500 mM imidiazole fraction from mock-transfected cell extracts was performed as a control; no peak of ATPase activity, with or without nucleic acid, could be detected across the mock gradient. No immunoreactive polypeptide was detected in the mock gradient fractions.

The peak glycerol gradient fractions were titrated for binding to RNA by the native gel mobility shift assay; the yield of the specific RNA-protein complex was linear with respect to input enzyme (Fig. 10A). The concentration of enzyme, expressed as RNA binding units, was 20 nM for wild-type His_{10}-NPH-II and 6 nM for His_{10}-NPH-II(H299A). ATPase activity of wild-type His_{10}-NPH-II varied with enzyme concentration; the specific activity in the presence of DNA or RNA cofactors was 12-fold higher than that in the absence of nucleic acid (Fig. 10B). In contrast, the activity of the H299A mutant was nucleic acid independent (Fig. 10C). The specific ATPase activity (per RNA binding unit) of His_{10}-NPH-II(H299A) was fivefold higher than that of the wild-type enzyme without cofactor and nearly half of that of the wild-type enzyme in the presence of DNA or RNA. Thus, the H299A substitution in the DExH box elicited a gain of function and uncoupled ATP hydrolysis from nucleic acid binding.

The enhanced nucleic acid-independent ATPase of the H299A mutant could be caused either by a decrease in the *K*m for NTP in the absence of nucleic acid or by an increase in the V_{max}. To discriminate between these possibilities, we analyzed the kinetic parameters for ATP hydrolysis for the wild-type and H299A proteins in the presence and absence of a DNA cofactor. ATP hydrolysis was determined as a function of ATP concentration in the range of 0.1 to 2 mM. K_m and V_{max} were derived from double-reciprocal plots of the data (not shown). The K_m values of the wild-type and H299A proteins in presence of DNA were virtually identical (1.15 ± 0.1 and 1.15 ± 0.07 mM, respectively [averages ± standard deviations for three separate experiments]). In the absence of a nucleic acid cofactor, the K_m values of the wild-type and H299A proteins were again essentially identical (0.36 ± 0.02 and 0.28 ± 0.03 mM, respectively [averages ± standard deviations for three separate experiments]). The observed K_m values for NTP in the presence of a nucleic acid cofactor agree with those reported for NPH-II purified from vaccinia virus virions (24). These results showed that the H299A mutation did not alter the affinity of the mutant protein for ATP. (The K_m for ATP

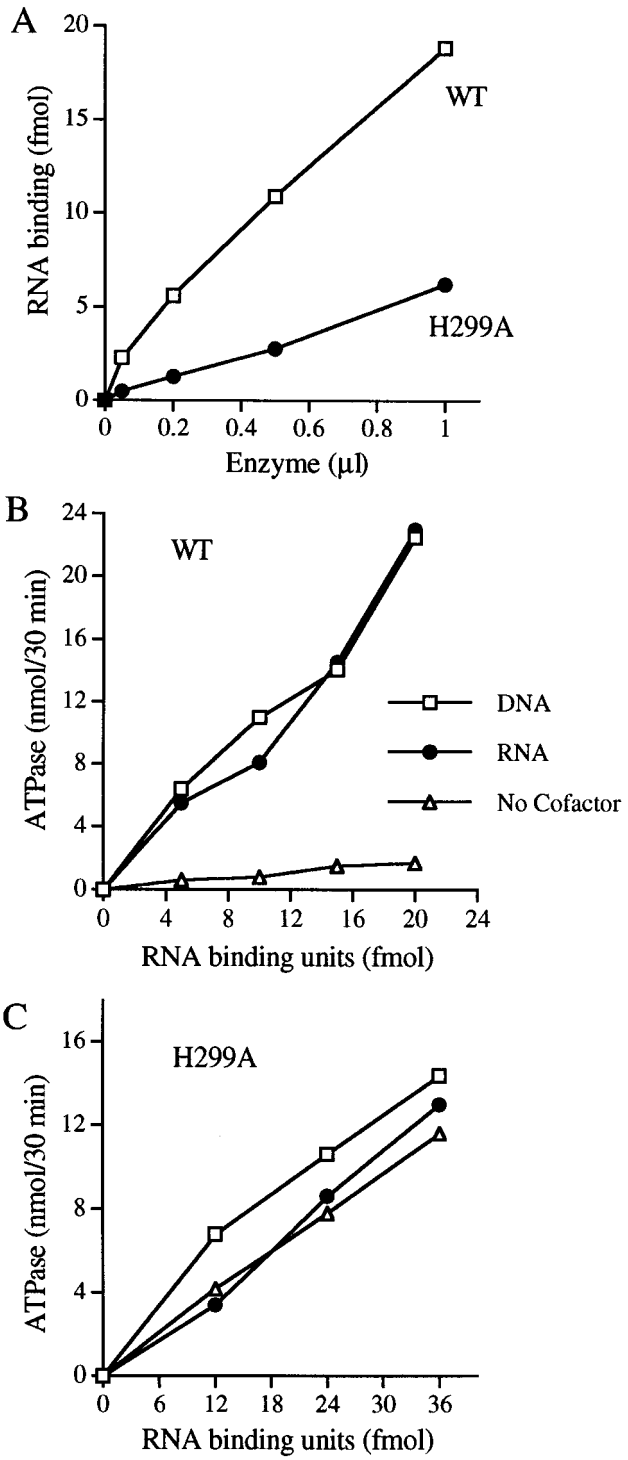

FIG. 10. RNA binding and ATPase activities of His_{10}-NPH-II proteins. (A) RNA binding assay mixtures contained the indicated volumes of the peak glycerol gradient fractions of wild-type (WT) and H299A proteins. The extent of RNA binding for each reaction was quantitated with a Phosphorimager. (B and C) ATPase activity in the presence of M13mp18 (DNA) or poly(C) (RNA) cofactor and in the absence of nucleic acid (No Cofactor) is plotted as a function of input enzyme for the wild-type (B) and H299A mutant (C) His_{10}-NPH-II proteins.

actually increased by about threefold in the presence of DNA; this was the case for both proteins.) The V_{max} of the wild-type His-NPH-II in the presence of a DNA cofactor was 41-fold higher than that in the absence of nucleic acid. In contrast, the V_{max} for the H299A protein with a DNA cofactor was only threefold higher than that in the absence of nucleic acid. Thus, the H299A mutation activated the nucleic acid-independent ATPase of NPH-II without affecting substrate affinity.

DISCUSSION

We have presented here an initial mutational analysis of vaccinia virus NPH-II, a DExH family member with bona fide RNA helicase activity. Our results underscore a direct correlation between the catalytic power of NPH-II in NTP hydrolysis and the efficiency of RNA unwinding. At the same time, we show that NTPase activity is insufficient to elicit strand displacement—chemical energy must be harnessed or coupled to helicase action. The His residue of the DExH box plays an essential role in this coupling process.

It is instructive to compare our results with those from the mutational and functional analyses of other helicases. Because the Walker A motif GxxGxGK(T/S) is common to so many proteins that bind and hydrolyze NTPs, and because crystallographic studies demonstrate that the invariant Lys makes direct contact with the β and γ phosphates of the bound nucleotide (23, 34), mutational studies of helicases have naturally focused on this lysine residue. Our finding that the K191A mutation of vaccinia virus NPH-II strongly suppresses NTP hydrolysis is not surprising and agrees with the effects of mutations at the corresponding residue in the eIF-4A (27), RAD3 (36), PriA (40), and UvrD (9) helicases.

The first Asp residue of the Walker B motif (analogous to the DExH box) interacts, via a water molecule, with a magnesium ion complexed with the β and γ phosphates of the bound nucleotide (23). We find that alanine substitutions at D-296 and E-297 in the DEVH box of NPH-II strongly reduce the NTPase and helicase activities. Pause and Sonenberg described similar effects of mutations at corresponding residues of eIF-4A, the prototypical RNA helicase of the DEAD box family (27). Conservative alterations in the DEAD box of eIF-4A to NEAD or DQAD abolished ATP hydrolysis and unwinding activities. Changing the eIF-4A DEAD box to EEAD abolished helicase activity with no effect on ATP hydrolysis (27). Thus, for eIF-4A, and for vaccinia virus NPH-II, helicase and ATPase activities can be uncoupled by specific changes in the DEAD or DExH boxes.

The effect of eliminating the histidine side chain in the DExH box of NPH-II is to constitutively activate NTPase, without need for a nucleic acid cofactor. Because wild-type NPH-II does display a low basal rate of NTP hydrolysis without a cofactor (this applies to the native enzyme from virions as well as the recombinant protein), it is axiomatic that the interaction of NPH-II with polynucleotides must accelerate the rate-limiting step in the NTPase cycle. The rate-limiting steps under single-turnover and steady-state conditions have not been determined for NPH-II (or, to our knowledge, for any other DExH or DEAD protein). The H299A mutant can bind stably to RNA, and yet its ATPase is not stimulated appreciably by RNA. Thus, whatever rate-enhancing conformational effect is elicited in the wild-type enzyme by RNA binding would essentially preexist in the H299A mutant. If RNA binding causes the position of the His-299 residue to change relative to the ground state (in order to relieve a suppressive effect of this moiety on the rate of hydrolysis), the elimination of the side chain by Ala substitution would be expected to mimic the

action of RNA, as we have observed. If helicase activity normally entails conformational cycling of the protein bound to the RNA 3′ tail, presumably coordinated with conversion of NTP to NDP, then the absence of such cycling in the constitutively active H299A NTPase when bound to RNA might account for the low efficiency of RNA unwinding by this protein. In this vein, it is noteworthy that changing the DEAD box motif in eIF-4A to DEAH had the effect of stimulating the rate of ATP hydrolysis while reducing RNA unwinding by an order of magnitude (27). Since wild-type eIF-4A displays no detectable ATPase in the absence of a polynucleotide cofactor (27), the ATPase activities of the eIF-4A mutants were determined by Pause and Sonenberg in the presence of poly(U). It would be of interest to determine if elimination of the side chain of the Asp residue in the DEAD box would constitutively activate the ATPase of eIF-4A, as we have observed for the His moiety in the DExH protein NPH-II.

Our mutational studies raise an issue of broad significance in the evaluation of other members of the DExH and DEAD box families; i.e., if variations at single residues can uncouple the NTPase and helicase activities, it may be unwarranted to assume that all DEAD and DExH family members are, in fact, helicases. The unifying theme based on the available biochemical evidence is that these proteins catalyze NTP hydrolysis in the presence of a nucleic acid cofactor. Failure to demonstrate helicase activity with standard screening assays is often rationalized by hypothetical requirements for additional protein cofactors or for highly specific nucleic acid structures as helicase substrates. While this may apply in some cases, it is worth considering that proteins of this type may couple the energy of NTP hydrolysis to events other than the unwinding of duplex nucleic acids.

Finally, although the initial mutational studies of a DExH box RNA helicase presented here are broadly consonant with the studies of eIF-4A, a DEAD box protein, it is worth mentioning that the properties of NPH-II differ significantly from those of eIF-4A. eIF-4A unwinds RNA bidirectionally, is ATP specific, requires a protein cofactor (eIF-4B), requires large molar excesses of both polypeptides to elicit strand displacement, and appears to require prior binding of ATP in order to bind to RNA (26–28). The properties of the vaccinia virus RNA helicase are most similar to those of human helicase A, a 3′-to-5′ RNA helicase that catalytically unwinds 3′-tailed RNA duplexes but is inactive with duplex DNAs (19). We anticipate that expanding the mutational analysis of NPH-II to the other conserved motifs will illuminate structure-function relationships common to both the DEAD and DExH families while providing some insight into the basis for those properties that are unique to NPH-II.

ACKNOWLEDGMENTS

This work was supported by American Cancer Society grants FRA-432 (to S.S.) and PF-4043 (to C.H.G.) and by NIH grant GM42498.

REFERENCES

1. **Bennett W. F., N. F. Paoni, B. A. Keyt, D. Botstein, A. J. Jones, L. Presta, F. M. Wurm, and M. J. Zoller.** 1991. High resolution analysis of functional determinants on human tissue-type plasminogen activator. J. Biol. Chem. **266:**5191–5201.
2. **Broyles, S. S., and B. Moss.** 1988. DNA-dependent ATPase activity associated with vaccinia virus early transcription factor. J. Biol. Chem. **263:**10761–10765.
3. **Burgess, S., J. R. Couto, and C. Guthrie.** 1990. A putative ATP binding protein influences the fidelity of branchpoint recognition in yeast splicing. Cell **60:**705–717.
4. **Chen, J.-H., and R.-J. Lin.** 1990. The yeast PRP2 protein, a putative RNA-dependent ATPase, share extensive sequence homology with two other pre-mRNA splicing factors. Nucleic Acids Res. **18:**6447.
5. **Company, M., J. Arenas, and J. Abelson.** 1991. Requirement of the RNA helicase-like protein PRP22 for release of messenger RNA from spliceosomes. Nature (London) **349:**487–493.
6. **Cunningham, B. C., and J. A. Wells.** 1989. High-resolution epitope mapping of hGH-receptor interactions by alanine-scanning mutagenesis. Science **244:**1081–1085.
7. **Elroy-Stein, O., T. R. Fuerst, and B. Moss.** 1989. Cap-independent translation of mRNA conferred by encephalomyocarditis virus 5′ sequence improves the performance of the vaccinia virus/bacteriophage T7 hybrid expression system. Proc. Natl. Acad. Sci. USA **86:**6126–6130.
8. **Fuerst, T. R., E. G. Niles, F. W. Studier, and B. Moss.** 1986. Eukaryotic transient-expression system based on recombinant vaccinia virus that synthesizes bacteriophage T7 RNA polymerase. Proc. Natl. Acad. Sci. USA **83:**8122–8126.
9. **George, J. W., R. M. Brosh, and S. W. Matson.** 1994. A dominant negative allele of the *Escherichia coli* uvrD gene encoding DNA helicase II. J. Mol. Biol. **235:**424–435.
10. **Gibbs, C. S., and M. J. Zoller.** 1991. Rational scanning mutagenesis of a protein kinase identifies functional regions involved in catalysis and substrate interactions. J. Biol. Chem. **266:**8923–8931.
11. **Gorbalenya, A. E., and E. V. Koonin.** 1993. Helicases: amino acid sequence comparisons and structure-function relationships. Curr. Opin. Struct. Biol. **3:**419–429.
12. **Guzder, S. N., P. Sung, V. Bailly, L. Prakash, and S. Prakash.** 1994. RAD25 is a DNA helicase required for DNA repair and RNA polymerase II transcription. Nature (London) **369:**578–581.
13. **Kim, S.-H., J. Smith, A. Claude, and R.-J. Lin.** 1992. The purified yeast pre-mRNA splicing factor PRP2 is an RNA-dependent NTPase. EMBO J. **11:**2319–2326.
14. **Koonin, E. V., and T. G. Senkevich.** 1992. Vaccinia virus encodes four putative DNA and/or RNA helicases distantly related to each other. J. Gen. Virol. **73:**989–993.
15. **Kunkel, T. A., J. D. Roberts, and R. A. Zakour.** 1987. Rapid and efficient site-specific mutagenesis without phenotypic selection. Methods Enzymol. **154:**367–403.
16. **Kuroda, M. I., M. J. Kernan, R. Kreber, B. Ganetzky, and B. S. Baker.** 1991. The *maleless* protein associates with the X chromosome to regulate dosage compensation in *Drosophila*. Cell **66:**935–947.
17. **Lain, S., J. L. Riechman, and J. A. Gracia.** 1990. RNA helicase: a novel activity associated with a protein encoded by a positive strand RNA virus. Nucleic Acids Res. **18:**7003–7006.
18. **Laurent, B. C., I. Triech, and M. Carlson.** 1993. The yeast SNF2/SWI2 protein has DNA-stimulated ATPase activity required for transcriptional activation. Genes Dev. **7:**583–591.
19. **Lee, C., and J. Hurwitz.** 1992. A new RNA helicase isolated from HeLa cells that catalytically translocates in the 3′ to 5′ direction. J. Biol. Chem. **267:**4398–4407.
20. **Lee, C.-G., and J. Hurwitz.** 1993. Human RNA helicase A is homologous to the maleless protein of *Drosophila*. J. Biol. Chem. **268:**16822–16830.
21. **Lee, M. S., and K. J. Marians.** 1990. Differential ATP requirements distinguish the DNA translocation and DNA unwinding activities of the *Escherichia coli* Pri A protein. J. Biol. Chem. **265:**17078–17083.
22. **Lloyd, R. G., and G. J. Sharples.** 1993. Dissociation of synthetic Holliday junctions by E. coli RecG protein. EMBO J. **12:**17–22.
23. **Pai, E. F., U. Krengel, G. A. Petsko, R. S. Goody, W. Kabsch, and A. Wittinghofer.** 1990. Refined crystal structure of the triphosphate conformation of H-ras p21 at 1.35 A resolution: implications for the mechanism of GTP hydrolysis. EMBO J. **9:**2351–2359.
24. **Paoletti, E., and B. Moss.** 1974. Two nucleic acid-dependent nucleoside triphosphate phosphohydrolases from vaccinia virus. Nucleotide substrate and polynucleotide cofactor specificities. J. Biol. Chem. **249:**3281–3286.
25. **Paoletti, E., H. Rosemond-Hornbeak, and B. Moss.** 1974. Two nucleic acid-dependent nucleoside triphosphate phosphohydrolases from vaccinia virus: purification and characterization. J. Biol. Chem. **249:**3273–3280.
26. **Pause, A., N. Méthot, and N. Sonenberg.** 1993. The HRIGRXXR region of the DEAD box RNA helicase eukaryotic translation initiation factor 4A is required for RNA binding and ATP hydrolysis. Mol. Cell. Biol. **13:**6789–6798.
27. **Pause, A., and N. Sonenberg.** 1992. Mutational analysis of a DEAD box RNA helicase: the mammalian translation initiation factor eIF-4A. EMBO J. **11:**2643–2654.
28. **Rozen, F., I. Edery, K. Meerovitch, T. E. Dever, W. C. Merrick, and N. Sonenberg.** 1990. Bidirectional RNA helicase activity of eucaryotic translation initiation factors 4A and 4F. Mol. Cell. Biol. **10:**1134–1144.
29. **Schmid, S. R., and P. Linder.** 1992. D-E-A-D protein family of putative RNA helicases. Mol. Microbiol. **6:**283–292.
30. **Schwer, B., and C. Guthrie.** 1991. PRP16 is an RNA-dependent ATPase that interacts transiently with the spliceosome. Nature (London) **349:**494–499.
31. **Shuman, S.** 1992. Vaccinia virus RNA helicase: an essential enzyme related to the DE-H family of RNA-dependent NTPases. Proc. Natl. Acad. Sci. USA **89:**10935–10939.

32. **Shuman, S.** 1993. Vaccinia virus RNA helicase. J. Biol. Chem. **268:**11798–11802.
33. **Shuman, S., E. Spencer, H. Furneaux, and J. Hurwitz.** 1980. The role of ATP in *in vitro* vaccinia virus RNA synthesis. J. Biol. Chem. **255:**5396–5403.
34. **Story, R. M., and T. A. Steitz.** 1992. Structure of the recA protein-ADP complex. Nature (London) **355:**374–376.
35. **Sung, P., V. Bailly, C. Weber, L. H. Thompson, L. Prakash, and S. Prakash.** 1993. Human xeroderma pigmentosum group D encodes a DNA Helicase. Nature (London) **365:**852–855.
36. **Sung, P., D. Higgins, L. Prakash, and S. Pakash.** 1988. Mutation of lysine-48 to arginine in the yeast RAD3 protein abolishes its ATPase and DNA helicase activities but not the ability to bind ATP. EMBO J. **7:**3263–3269.
37. **Sung, P., L. Prakash, S. W. Matson, and S. Prakash.** 1987. RAD3 protein of *Saccharomyces cerevisiae* is a DNA helicase. Proc. Natl. Acad. Sci. USA **84:**8951–8955.
38. **Umezu, K., and H. Nakayama.** 1990. *Escherichia coli* RecQ protein is a DNA helicase. Proc. Natl. Acad. Sci. USA **87:**5363–5367.
39. **Walker, J. E., and M. Saraste, M. J. Runswick, and N. J. Gay.** 1982. Distantly related sequences in the a- and b-subunits of ATP synthetase, myosin, kinases and other ATP-requiring enzymes and a common nucleotide binding fold. EMBO J. **1:**945–951.
40. **Zavitz, K. H., and K. J. Marians.** 1987. ATPase-deficient mutants of the *Escherichia coli* DNA replication protein PriA are capable of catalyzing the assembly of active primosomes. J. Biol. Chem. **267:**6933–6940.